



Article

Stability and Sensitivity Analysis of the COVID-19 Spread with Comorbid Diseases

Jonner Nainggolan ^{1,*} 0000-0001-7250-4521, Moch. Fandi Ansori ² 0000-0002-4588-3885

¹ Department of Mathematics, Faculty of Mathematics and Natural Sciences, Universitas Cenderawasih, Jayapura, Indonesia, 99224
² Department of Physics Faculty of Science and Mathematics, Universitas Diponegoro, Jl. Prof. Jacob Rais, Semarang, Indonesia, 50275
* Correspondence: jonner2766@gmail.com

Abstract: This research investigates a model of the spread of COVID-19 in Indonesia by paying attention to comorbid disease, self-quarantine, government-provided quarantine, and vaccination factors. The symmetrical aspects of the model are studied. Evaluation of the model reveals non-endemic and endemic equilibrium points, and the basic reproduction number (BRN). We provide the local and global stability analysis of the equilibriums. According to the sensitivity analysis of the BRN, the key parameters impacting the spread of COVID-19 are susceptible recruitment rate, contact rate, infection death rate, and probability of infected individuals having no comorbidities. In addition, we provide sensitivity analysis to examine the effect of parameter changes on each subpopulation. We discovered that the natural death rate is the most sensitive parameter based on the sensitivity index after reaching equilibrium. Symmetry aspects appear in some of the visualization of the model’s solution and the sensitivity of BRN and parameters.

Keywords: mathematical model; COVID-19; comorbid disease; sensitivity analysis; basic reproduction number.

MSC: 37N25; 93B35

1. Introduction

COVID-19 is an illness caused by severe acute respiratory syndrome coronavirus 2 infection (SARS-CoV-2). The illness can induce a range of respiratory system problems from mild symptoms like the flu to severe lung infections like pneumonia [1]. Antiviral medicines and vaccines for COVID 19 prevention were identified in 2021. In order to combat COVID-19, health professionals and mathematicians can work together to analyze, evaluate, anticipate, and optimize the prevention strategies. For examples, mathematical models can be utilized to analyze COVID-19 preventive with less effective vaccines [2], to study the vaccine and treatment for the disease [3,4], and to examine the optimal control to combat the spread of the disease [5–9].

There are many approaches for modelling the COVID-19 spread by considering various factors. Ahmed et. al. [10] analyzed the COVID-19 model with numerical analysis and logistic model. Arino and Portet [11] proposed the COVID-19 model by taking into account susceptible, latently infected, symptomatic and asymptomatic infectious, and recovered individuals. Arfan et. al. [12] investigated a fractional dynamical system of COVID-19 based on modified susceptible-exposed-infectious-recovered type with nonsingular kernel derivative. Arfan et. al. [13] examined the non-integer order population dynamical model of the COVID-19 pandemic in relation to various values of the heavily impacted system parameter of immigration for both susceptible and infected populations. Sugiyanto and Abrori [14] studied the model of COVID-19 spread by considering the case of with and without lockdown. Khan et. al. [15] considered the model of COVID-19 dynamics where the infected subpopulations having isolation and quarantined.

Several researchers have studied models of the COVID-19 spread in different parts of the world. Annas et. al. [16] analyzed and provided numerical simulations for the model of COVID-19 spread susceptible-exposed-infectious-recovered type in Indonesia. Fitriani et. al. [17] studied the dynamic of COVID-19 transmission in Central Java, Indonesia. Anggriani et. al. [18] investigated the model of COVID-19 propagation in West Java, Indonesia. Okuonghae and Oname [19] reviewed the model of COVID-19 contagion in Lagos, Nigeria. Kifle and Obsu [20] considered the model of COVID-19 infectious in Ethiopia between March 2020 and July 2021. Asempapa et. al. [21] studied the model of COVID-19 spread in Brazil and South Africa among populations at risk of death through the provision of natural medicine preventatives.

Various attempts have been made to estimate the data of COVID-19 cases in order to predict its spread. Postnikov [22] studied the criteria for predicting the COVID-19 spread using susceptible-infectious-recovered type model. Using data provided in China, Macau, Hong Kong, and Taiwan, Ivorra et. al. [23] determined the characteristics of the COVID-19 model which is used to predict the disease transmission in other countries and also in Wuhan, China as used by Yang and Wang [24]. Barmparis and Tsironis [25] provided an estimation technique of COVID-19 distribution parameters using data from nine nations. Sreeramula and Rahardjo [26] presented an estimation of COVID-19 propagation parameters in Indonesia.

Modelling the COVID-19 transmission in relation to other diseases can give rich examination to the infectious dynamics characteristics. Mekonen et. al. [27] evaluated the model for the spread of tuberculosis coinfectd with COVID-19. Ssebuliba et. al. [28] studied the COVID-19 contagion by considering the infected individuals having partially comorbid diseases. In [29,30], the COVID-19 spread is examined where the individuals with comorbid diseases having interventions of natural remedies and vaccination. Okyere and Ackora-Prah [31] analyzed the COVID-19 transmission dynamics by taking into account of diabetes.

In the dynamic model of COVID-19 spread studied by Ssebuliba et. al. [28], individuals infected with COVID-19 with or without comorbid diseases are shifted to the hospital (local government quarantine) without reference to the self-quarantine in their respective homes. On the basis of Ssebuliba et. al. [28] model, in this paper, we extend the model by taking into account the transfer rate from individuals infected with COVID-19 without comorbid disease to the self-quarantine individuals. This is important to note because, according to real data from Indonesia, individuals infected with COVID-19 without comorbid diseases are generally isolated in their respective homes because they can recover by consuming nutritious foods, taking vitamins, getting enough rest, exercising, and adhering to health protocols [1]. The symmetrical aspects for the dynamical system are analyzed, such as the non-endemic and endemic equilibrium points and their stability, and also the basic reproduction number. We perform some numerical simulations to visualize the solution of the system, the sensitivity analysis of the basic reproduction number to study the stability of the system, and the sensitivity of the model's parameters to study their effects on the solution of the system. The symmetry appears in some of these visualizations. Based on the sensitivity index after reaching equilibrium, we determine which parameter that is the most sensitive.

2. The Spread of COVID-19 with Comorbid Diseases

Consider a population which is divided into six subpopulations. S denotes the susceptible subpopulation which consists of individuals who are still healthy but susceptible to infection of COVID-19. I_h denotes the subpopulation which is infected with COVID-19 but have no comorbid diseases. I_c denotes the subpopulation which is infected with COVID-19 and has a history of comorbid diseases such as hypertension, diabetes mellitus, heart disease, respiratory disorders, chronic renal disease, neurological disorders, endocrine disorders, and liver. Q_h represents the self-quarantine subpopulation which consists of persons infected with COVID-19 without comorbid diseases. Q_H represents the subpopu-

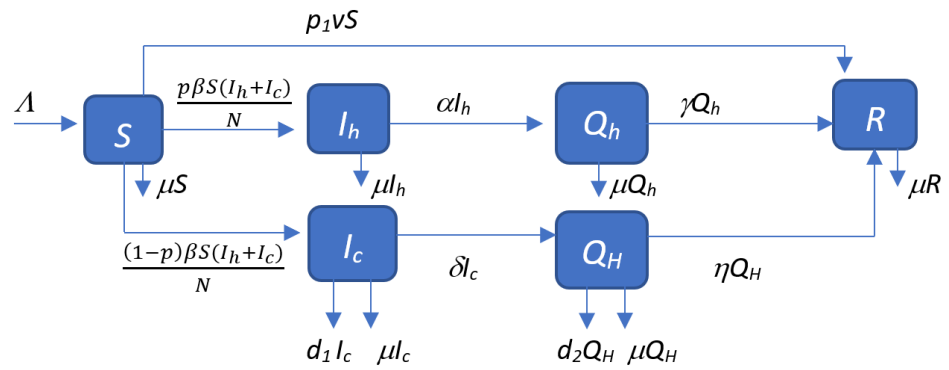


Figure 1. Schematic diagram of the spread of COVID-19 with regard to comorbid diseases.

lation of COVID-19-infected persons with comorbid diseases who are isolated in a local government-supplied quarantine. R represents the recovered subpopulation which consists of individuals who have recovered from or are immune to COVID-19.

The following are the model's underlying assumptions: (1) New recruits are introduced into the susceptible subpopulation. (2) Individuals from the susceptible subpopulation who are immunized against COVID-19 and enter the recovered subpopulation. (3) Susceptible subpopulation who come in contact with COVID-19-infected individuals become infected. (4) COVID-19-infected individuals who do not have comorbid diseases are self-quarantined in their residences. (5) Individuals infected with COVID-19 and comorbid diseases are quarantined in a local government-provided facility. (6) Each subpopulation died of natural causes. (7) The majority of individuals who received treatment or supplements healed. (8) Those infected with COVID-19 may perish. Schematic representation of the spread of COVID-19 by paying attention to comorbid diseases is depicted in Fig. 1.

On the basis of the assumptions and the schematic diagram in Fig. 1, the following system of differential equations is derived,

$$\left\{ \begin{array}{l} \frac{dS}{dt} = \Lambda - \frac{\beta S(I_h + I_c)}{N} - (p_1v + \mu)S \\ \frac{dI_h}{dt} = \frac{p\beta S(I_h + I_c)}{N} - (\alpha + \mu)I_h \\ \frac{dI_c}{dt} = \frac{(1-p)\beta S(I_h + I_c)}{N} - (d_1 + \delta + \mu)I_c \\ \frac{dQ_h}{dt} = \alpha I_h - (\gamma + \mu)Q_h \\ \frac{dQ_H}{dt} = \delta I_c - (d_2 + \eta + \mu)Q_H \\ \frac{dR}{dt} = p_1vS + \gamma Q_h + \eta Q_H - \mu R \end{array} \right. \quad (1)$$

The description of the parameters of system (1) are presented in Table 1. Their value are derived in part from Indonesian journals, calculated based on data from the Ministry of Health of the Republic of Indonesia, and assumed in minor part.

3. Model Analysis

The total population is bounded at any time $t > 0$. The following lemmas show that the solution of system (1) is bounded.

Lemma 1. The feasible region Ω defined by $\Omega = \{(S(t), I_h(t), I_c(t), Q_h(t), Q_H(t), R(t)) \in \mathbb{R}_+^6 \mid 0 < N(t) \leq \max\{N(0), \Lambda/\mu\}, \text{ with initial conditions } S(t) \geq 0, I_h(t) \geq 0, I_c(t) \geq 0, Q_h(t) \geq 0, Q_H(t) \geq 0, R(t) \geq 0, \text{ is non-negative invariant and associated with equation (1) for } t > 0.$

Table 1. Description of the parameters and their value.

Parameters	Description	Value	Source
Λ	Recruitment rate of individuals entering the susceptible subpopulation	4589	[1]
p	Probability of infected individuals entering the I_h subpopulation	0.65	Estimated
β	Individual contact rate of the susceptible subpopulation with the infected subpopulations	0.036	[14]
ν	Individual rate of the susceptible subpopulation being vaccinated	0.1	[16]
p_1	Chances of vaccine effectiveness	0.55	Estimated
μ	Natural death rate of each subpopulation	$\frac{1}{65 \times 365}$	Estimated
α	Individual transfer rates from the I_h to Q_h subpopulations	0.2143	Assumed
d_1	Death rate of individuals infected with COVID-19	7.344×10^{-7}	[16]
δ	Individual transfer rates from subpopulation I_c to Q_H	0.0714	Assumed
γ	Recovery rate of individuals who are infected with COVID-19 but have no comorbidities	0.003065	Estimated
d_2	Death rate of individuals infected with COVID-19 and having comorbid diseases	0.0177	[1]
η	Recovery rate of individuals infected with COVID-19 and having comorbid diseases	0.00124	[1]

Proof. Equation dS/dt in (1), for all $t > 0$, can show the change in the number of susceptible per time,

$$\frac{dS}{dt} \geq \frac{p\beta S(I_h + I_c)}{N} + \frac{(1-p)\beta S(I_h + I_c)}{N} + (\nu + \mu)S = -\left(\frac{\beta(I_h + I_c)}{N} + \nu + \mu\right)S.$$

By taking the limit $t \rightarrow \infty$ on both sides, we obtain

$$S(t) \geq S_0 \exp\left(-\left[\mu t + \int_0^t \frac{\beta(I_h(k) + I_c(k))}{N} dk\right]\right),$$

and therefore

$$\liminf_{t \rightarrow \infty} S(t) \geq 0.$$

Similarly, it can be shown that $I_h(t) \geq 0$, $I_c(t) \geq 0$, $Q_h(t) \geq 0$, $Q_H(t) \geq 0$, $R(t) \geq 0$. When all initial conditions are non-negative, it can be shown that the solutions of system (1) are non-negative. \square

Lemma 2. Solutions of system (1) are bounded for all $t \in [0, t_1]$.

Proof. The change in total population per unit time is

$$\frac{dN}{dt} = \Lambda - d_1 I_c - d_2 Q_H - \mu N.$$

Therefore, the total population is bounded, that is

$$0 \leq \limsup_{t \rightarrow \infty} N(t) \leq \frac{\Lambda}{\mu}.$$

This indicates that all solutions of system (1) are bounded for all $t \in [0, t_1]$. \square

3.1. Non-endemic Equilibrium Point

The necessary and sufficient conditions for obtaining a non-endemic equilibrium point are the number of changes in subpopulations per unit time is constant, and the number of individuals confirmed positive for COVID-19 and the number of individuals quarantined are both zero. From (1), by setting $\frac{dS}{dt} = \frac{dI_h}{dt} = \frac{dI_c}{dt} = \frac{dQ_h}{dt} = \frac{dQ_H}{dt} = \frac{dR}{dt} = 0$ and $I_h = I_c = Q_h = Q_H = 0$, we obtain the non-endemic equilibrium point as follows

$$E_1 = (S_1^*, I_{h1}^*, I_{c1}^*, Q_{h1}^*, Q_{H1}^*, R_1^*) = \left(\frac{\Lambda}{\mu}, 0, 0, 0, 0, \frac{v\Lambda}{\mu(v+\mu)} \right). \quad (2)$$

The local stability of the non-endemic equilibrium is given below.

Theorem 1. *The non-endemic equilibrium point E_1 is locally asymptotically stable.*

Proof. In the manner used by Diekmann and Heesterbeek [32], by substituting the non-endemic equilibrium point in the Jacobian matrix of system (1), we get

$$J(E_1) = \begin{bmatrix} -p_1v - \mu & -k & -k & 0 & 0 & 0 \\ 0 & pk - \alpha - \mu & pk & 0 & 0 & 0 \\ 0 & (1-p)k & (1-p)k - d_1 - \delta - \mu & 0 & 0 & 0 \\ 0 & \alpha & 0 & -\gamma - \mu & 0 & 0 \\ 0 & 0 & \delta & 0 & -d_2 - \eta - \mu & 0 \\ p_1v & 0 & 0 & \gamma & \eta & -\mu \end{bmatrix},$$

with $k = \frac{\beta\Lambda}{\mu N}$. Eigen values of the Jacobian matrix $J(E_1)$ are $\lambda_1 = -\mu$, $\lambda_2 = -p_1v - \mu$, $\lambda_3 = -d_2 - \eta - \mu$, $\lambda_4 = -\gamma - \mu$, $\lambda_5 = -\frac{1}{2}(\alpha + d_1 + \delta - 2\mu) + \frac{1}{2}k - \frac{1}{2}\sqrt{A}$, $\lambda_6 = -\frac{1}{2}(\alpha + d_1 + \delta - 2\mu) + \frac{1}{2}k + \frac{1}{2}\sqrt{A}$, where

$$A = 4kp(d_1 + \delta - \alpha) + (\alpha - d_1)^2 + 2\alpha(k - \delta) + d_1(d_1 + 2\delta - 2k) + (\delta - k)^2.$$

Since it can be observed that $\lambda_i < 0$, $i = 1, 2, 3, 4, 5$, and λ_6 will be negative if

$$\frac{1}{2}(kp + \alpha + d_1) + \mu > d + \frac{1}{2}\sqrt{A}, \quad (3)$$

then the equilibrium point E_1 is asymptotically stable if (3) is fulfilled. \square

3.2. The Basic Reproduction Number

The basic reproduction number is an essential indicator for determining whether the rate of disease transmission is rising or decreasing. The basic reproduction number is usually denoted by R_0 . The interpretation is that if $R_0 > 1$ then the disease is increasing, and if $R_0 < 1$ then the disease is decreasing or disappearing. Based on the system (1), the basic reproduction number can be determined using the next-generation matrix [33]. The Jacobian matrix, taking into account the susceptible subpopulation in contact with the infected, denoted by J_G , is give as follows

$$J_G = \frac{1}{N} \begin{bmatrix} \beta(I_h + I_c) & -\beta S & -\beta S \\ p\beta(I_h + I_c) & p\beta S & p\beta S \\ (1-p)\beta(I_h + I_c) & (1-p)\beta S & (1-p)\beta S \end{bmatrix}.$$

Evaluating J_G at the non-endemic equilibrium results

$$G_F := J_G(E_1) = \begin{bmatrix} 0 & -\frac{\beta\Lambda}{\mu N} & -\frac{\beta\Lambda}{\mu N} \\ 0 & \frac{p\beta\Lambda}{\mu N} & \frac{p\beta\Lambda}{\mu N} \\ 0 & \frac{(1-p)\beta\Lambda}{\mu N} & \frac{(1-p)\beta\Lambda}{\mu N} \end{bmatrix}.$$

The jacobian matrix of susceptible and infected subpopulations that enter and are contactless is

$$G_V = \begin{bmatrix} p_1\nu + \mu & 0 & 0 \\ 0 & \alpha + \mu & 0 \\ 0 & 0 & d_1 + \delta + \mu \end{bmatrix}.$$

Eigen values of $G_F G_V^{-1}$ are $\lambda_1 = 0, \lambda_2 = 0, \lambda_3 = \frac{\beta\Lambda[p(d_1+\delta-\alpha)+\alpha+\mu]}{\mu N(\alpha+\mu)(d_1+\delta+\mu)}$. According to [33], the basic reproduction number of the system (1) is

$$R_0 = \frac{\beta\Lambda[p(d_1+\delta-\alpha)+\alpha+\mu]}{\mu N(\alpha+\mu)(d_1+\delta+\mu)}. \quad (4)$$

3.3. Endemic Equilibrium Point

125

The necessary conditions for obtaining the endemic equilibrium point of system (1) are $\frac{dS}{dt} = \frac{dI_h}{dt} = \frac{dI_c}{dt} = \frac{dQ_h}{dt} = \frac{dQ_{H2}}{dt} = \frac{dR}{dt} = 0$. The endemic equilibrium point is

$$E_2 = (S_2^*, I_{h2}^*, I_{c2}^*, Q_{h2}^*, Q_{H2}^*, R_2^*),$$

with

$$\begin{aligned} S_2^* &= \frac{k_2 k_3 N}{\beta[p(k_3 - k_2) + k_2]}, \\ I_{h2}^* &= \frac{p\beta\Lambda(k_2 - k_3) + k_2(k_1 k_3 N - \beta\Lambda)}{\beta k_2[p(k_2 - k_3) - k_2]}, \\ I_{c2}^* &= \frac{(1-p)[p\beta\Lambda(k_2 - k_3) + k_2(k_1 k_3 N - \beta\Lambda)]}{p\beta k_3[p(k_2 - k_3) - k_2]}, \\ Q_{h2}^* &= \frac{p\alpha\beta\Lambda(k_2 - k_3) + k_2(k_1 k_3 N - \beta\Lambda)}{\beta k_2 k_4[p(k_2 - k_3) - k_2]}, \\ Q_{H2}^* &= \frac{(1-p)\delta[p\beta\Lambda(k_2 - k_3) + \delta k_2(k_1 k_3 N - \beta\Lambda)]}{p\beta k_3 k_5[p(k_2 - k_3) - k_2]}, \\ R_2^* &= \frac{p_1 r S_2^* + \gamma Q_{h2}^* + \eta Q_{H2}^*}{\mu}, \end{aligned}$$

where $k_1 = p_1\nu + \mu, k_2 = \alpha + \mu, k_3 = d_1 + \delta + \mu, k_4 = \gamma + \mu, k_5 = d_2 + \eta + \mu$. 126

The local stability of the endemic equilibrium is provided below. 127

Theorem 2. The endemic equilibrium point E_2 is locally asymptotically stable. 128

Proof. By substituting the endemic equilibrium point E_2 into the Jacobian matrix of system (1), we obtain

$$J(E_2) = \begin{bmatrix} -\beta^* - p_1\nu - \mu & -\frac{\beta S_2^*}{N} & -\frac{\beta S_2^*}{N} & 0 & 0 & 0 \\ p\beta^* & \frac{p\beta S_2^*}{N} - \alpha - \mu & \frac{p\beta S_2^*}{N} & 0 & 0 & 0 \\ (1-p)\beta^* & \frac{(1-p)\beta S_2^*}{N} & \frac{(1-p)\beta S_2^*}{N} - d_1 - \delta - \mu & 0 & 0 & 0 \\ 0 & \alpha & 0 & -\gamma - \mu & 0 & 0 \\ 0 & 0 & \delta & 0 & -d_2 - \eta - \mu & 0 \\ p_1\nu & 0 & 0 & \gamma & \eta & -\mu \end{bmatrix},$$

where $\beta^* = \frac{\beta(I_{h2}^* + I_{c2}^*)}{N}$. 129

The characteristic polynomial of $J(E_2)$ is

$$\mathcal{P}(x) = \frac{1}{N^2}(\lambda_1 + \mu)(\lambda + \gamma + \mu)(\lambda + d_2 + \eta + \mu)\mathcal{G}(\lambda),$$

with $\lambda_1 = -\mu$, $\lambda_2 = -\gamma - \mu$, $\lambda_3 = -d_2 - \eta - \mu$, and

$$\mathcal{G}(\lambda) = \lambda^3 + c_1\lambda^2 + c_2\lambda + c_3, \quad (5)$$

where

$$\begin{aligned} c_1 &= \frac{1}{N}([(p+1)k_6 - p_1\nu + \alpha + k_3]N + \beta S_2^*(p-1)), \\ c_2 &= \left(\left[-pk_6^2 + ((p_1\nu - d_1 - \delta)p + k_2 + k_3)k_6 - \nu(\alpha + k_2 + k_3)p_1 + \alpha(\delta + d_1) - \mu^2 \right] N^2 \right. \\ &\quad \left. S_2^*[(2-p)pk_6 + (1-p)(p_1\nu - \alpha)]\beta N + p\beta^2 S_2^{*2}(p-1) \right) \frac{\lambda}{N^2}, \\ c_3 &= -\frac{1}{N^2} \left[k_3 N^2 (k_1 - k_6)(-pk_6 + k_2) - S_2^*[(p-1)\mu^2 + -p^2 k_6 + k_1(p-1)]\mu \right. \\ &\quad \left. - p^2 \nu k_6 p_1 + [(p_1\nu - d_1 - \delta)k_6 + \alpha p_1 \nu]p - \alpha p_1 \nu \beta N - p(p-1)\beta^2 S_2^{*2} k_1 \right], \end{aligned}$$

with $k_6 = \frac{\beta(I_{h2}^* + I_{c2}^*)}{N}$.

To show that the equilibrium point E_2 is locally asymptotically stable, we must prove that all roots of the polynomial (5) are negative. Based on the Routh-Hurwitz criteria, all roots of (5) are negative if they are fulfilled $c_1 > 0$, $c_2 > 0$, $c_3 > 0$ and $c_1 c_2 - c_3 > 0$. Using the parameter values in Table 1 and the initial subpopulation values S_2^* , I_{h2}^* , I_{c2}^* . We obtain $c_1 = 0.218156$, $c_2 = 0.01161589$, $c_3 = 0.00067804$, and we can verify that $c_1 c_2 - c_3 = 0.00185604$. This shows that $c_1 > 0$, $c_2 > 0$, $c_3 > 0$, and $c_1 c_2 - c_3 > 0$. Therefore, the endemic equilibrium point E_2 is locally asymptotically stable. \square

3.4. Global Stability Analysis

Following [34], the global stability of equilibrium point E_2 is analyzed. The expression of E_2 can be written as

$$\begin{aligned} \Lambda &= \frac{qS_2^*(I_{h2}^* + I_{c2}^*)}{N} + (p_1\nu + \mu)S_2^*, & I_{h2}^* &= \frac{S_2^* I_{c2}^*}{(\alpha + \mu)N - pqS_2^*}, \\ I_{c2}^* &= \frac{(1-p)qS_2^* I_{h2}^*}{(d_1 + \delta + \mu)N - (1-p)qS_2^*}, & (\gamma + \mu)Q_{h2}^* &= \alpha I_{h2}^*, \\ (d_2 + \eta + \mu)Q_{H2}^* &= \delta I_{c2}^*, & \mu R_2^* &= p_1\nu S_2^* + \gamma Q_{h2}^* + \eta Q_{H2}^*, \end{aligned}$$

with q is multiplication of a constant by the parameter β .

The global stability of the endemic equilibrium is given below.

Theorem 3. If $R_0 > 1$, then the endemic equilibrium E_2 is globally asymptotically stable.

Proof. Define a Lyapunov function

$$\begin{aligned} L &= \int_{S_2^*}^S \left(1 - \frac{S_2^*}{y}\right) dy + \int_{I_{h2}^*}^{I_{h2}} \left(1 - \frac{I_{h2}^*}{y}\right) dy + \int_{I_{c2}^*}^{I_{c2}} \left(1 - \frac{I_{c2}^*}{y}\right) dy \\ &\quad + \int_{Q_{h2}^*}^{Q_{h2}} \left(1 - \frac{Q_{h2}^*}{y}\right) dy + \int_{Q_{H2}^*}^{Q_{H2}} \left(1 - \frac{Q_{H2}^*}{y}\right) dy + \int_{R_2^*}^R \left(1 - \frac{R_2^*}{y}\right) dy. \end{aligned}$$

The first derivative of the Lyapunov function is given by

$$\begin{aligned} L' &= \left(1 - \frac{S_2^*}{S}\right) S'_2 + \left(1 - \frac{I_{h2}^*}{I_{h2}}\right) I'_{h2} + \left(1 - \frac{I_{c2}^*}{I_{c2}}\right) I'_{c2} + \left(1 - \frac{Q_{h2}^*}{Q_{h2}}\right) Q'_{h2} \\ &\quad + \left(1 - \frac{Q_{H2}^*}{Q_{H2}}\right) Q'_{H2} + \left(1 - \frac{R_2^*}{R}\right) R'_2, \end{aligned}$$

where

$$\begin{aligned}
 \left(1 - \frac{S_2^*}{S}\right) S_2' &= \left(1 - \frac{S_2^*}{S}\right) \left(\frac{qS_2^*(I_{h2}^* + I_{c2}^*)}{N} + k_1 S_2^* - \frac{\beta S(I_h + I_c)}{N} - k_1 S \right) \\
 &= (p_1\nu + \mu) S_2^* \left(2 - \frac{S}{S_2^*} - \frac{S_2^*}{S}\right) + \left(1 - \frac{S_2^*}{S}\right) \left[\frac{qS_2^*(I_{h2}^* + I_{c2}^*)}{N} - \frac{\beta S(I_h + I_c)}{N} \right], \\
 \left(1 - \frac{I_{h2}^*}{I_h}\right) I_{h2}' &= \left(1 - \frac{I_{h2}^*}{I_h}\right) \left(\frac{p\beta S(I_h + I_c)}{N} - k_2 I_h \right) \\
 &= \left(1 - \frac{I_{h2}^*}{I_h}\right) \left(\frac{p\beta S(S_2^* I_{c2}^* + [k_2 N - pqS_2^*]) I_c}{k_2 N^2 - pqNS_2^*} - \frac{k_2 S_2^* I_{c2}^*}{k_2 N - pqS_2^*} \right), \\
 \left(1 - \frac{I_{c2}^*}{I_c}\right) I_{c2}' &= \left(1 - \frac{I_{c2}^*}{I_c}\right) \left(\frac{(1-p)\beta S(I_h + I_c)}{N} - k_3 I_c \right) \\
 &= \left(1 - \frac{I_{c2}^*}{I_c}\right) \left(\frac{(1-p)\beta S(I_h + I_{h2}^*)}{N} - \frac{(1-p)qk_3 S_2^* I_{h2}^*}{k_3 N - (1-p)qS_2^*} \right), \\
 \left(1 - \frac{Q_{h2}^*}{Q_h}\right) Q_{h2}' &= \left(1 - \frac{Q_{h2}^*}{Q_h}\right) [\alpha I_h - (\gamma + \mu) Q_h] \\
 &= \left(1 - \frac{Q_{h2}^*}{Q_h}\right) \alpha \left(\frac{S_2^* I_{c2}^*}{k_2 N - pqS_2^*} - I_{h2}^* \right), \\
 \left(1 - \frac{Q_{H2}^*}{Q_H}\right) Q_{H2}' &= \left(1 - \frac{Q_{H2}^*}{Q_H}\right) (\delta I_c - k_3 Q_H) \\
 &= \left(1 - \frac{Q_{H2}^*}{Q_H}\right) \delta \left(\frac{(1-p)qS_2^* I_{h2}^*}{k_3 N - (1-p)qS_2^*} - I_{c2}^* \right), \\
 \left(1 - \frac{R_2^*}{R}\right) R_2' &= \left(1 - \frac{R_2^*}{R}\right) [p_1\nu(S - S_2^*) + \gamma(Q_h - Q_{h2}^*) + \eta(Q_H - Q_{H2}^*)].
 \end{aligned}$$

Then we have

$$\begin{aligned}
 L' &= \mu S_2^* \left(2 - \frac{S}{S_2^*} - \frac{S_2^*}{S}\right) + \frac{\beta}{N} \left(3 - \frac{S_2^*}{S} - \frac{I_h}{I_{h2}^*} - \frac{I_{h2}^* Q_h}{Q_{h2}^* I_h} - \frac{I_c}{I_{c2}^*} \left[\frac{S Q_{h2}^*}{S_2^* Q_h} - 1 \right] \right) \\
 &\quad + \frac{\beta}{N} \left(3 - \frac{S_2^*}{S} - \frac{I_c}{I_{c2}^*} - \frac{I_{c2}^* Q_H}{Q_{H2}^* I_c} - \frac{I_h}{I_{h2}^*} \left[\frac{S Q_{H2}^*}{S_2^* Q_H} - 1 \right] \right). \quad (6)
 \end{aligned}$$

From (6) we have

$$\begin{aligned}
 \mu S_2^* \left(2 - \frac{S}{S_2^*} - \frac{S_2^*}{S}\right) &\leq 0, \\
 \frac{\beta}{N} \left(3 - \frac{S_2^*}{S} - \frac{I_h}{I_{h2}^*} - \frac{I_{h2}^* Q_h}{Q_{h2}^* I_h} - \frac{I_c}{I_{c2}^*} \left[\frac{S Q_{h2}^*}{S_2^* Q_h} - 1 \right] \right) &\leq 0, \\
 \frac{\beta}{N} \left(3 - \frac{S_2^*}{S} - \frac{I_c}{I_{c2}^*} - \frac{I_{c2}^* Q_H}{Q_{H2}^* I_c} - \frac{I_h}{I_{h2}^*} \left[\frac{S Q_{H2}^*}{S_2^* Q_H} - 1 \right] \right) &\leq 0.
 \end{aligned}$$

Thus, the largest invariant subset is obtained $L' = 0$. By Lasalle's invariance principle [35], if $R_0 > 1$ then E_2 is globally asymptotically stable. \square

4. Result and Discussion

4.1. Numerical Solutions

The numerical simulations in this study uses the parameter values in Table 1, and the number of initial subpopulations in 2020 the spread of COVID-19 in Indonesia with the initial number of each subpopulation is $S(0) = 267823870$, $I_h(0) = 23601$, $I_c(0) = 3842$, $Q_h(0) = 8630$, $Q_H(0) = 2034$, $R(0) = 286$, $N = 268000000$. We solve the system (1) numerically by using Runge-Kutta order 45 method, in Matlab we use package function `ode45`. The graphs of the numerical solution of the system are given in Fig. 2. We group

the subpopulations S with R , I_h with I_c , and Q_h and Q_H , based on the value level and comparison meaning. Here we can observe that a symmetrical aspect appears in the susceptible and recovered subpopulations.

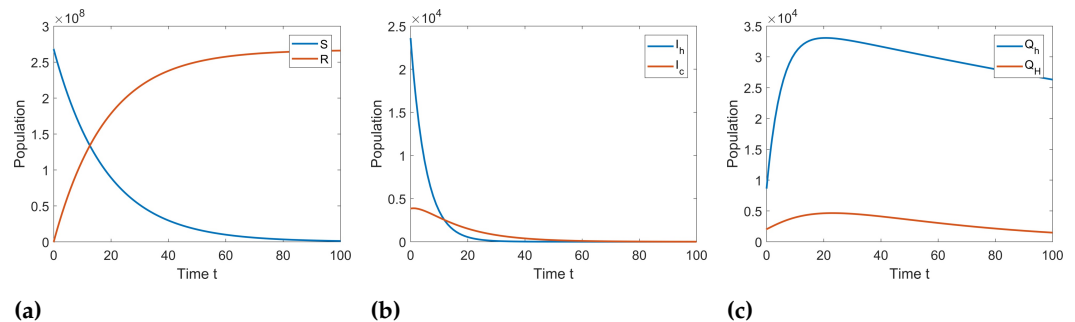


Figure 2. Numerical solution of the system (1). Panel (a) is for susceptible (S) and recovered (R) subpopulations, panel (b) is for infected without comorbid (I_h) and infected with comorbid (I_c) subpopulations, and panel (c) is for self-quarantine (Q_h) and local government-supplied quarantine (Q_H) subpopulations.

4.2. Basic Reproduction Number Sensitivity Analysis

The basic reproduction number R_0 in (4) can be viewed as a function of parameters. So, we can visualize R_0 as a function of two parameters by making other parameters as constant and then plot the graph. We have plotted the contour plots of R_0 function for every combination of two parameters appeared in (4), and most of them give results the contour of R_0 having value below 1. Only from the combination of parameters Λ , β , p , and d_1 , there can be seen the spectrum of R_0 value varying from below 1 until above 1, as shown in Fig. 3. We can conclude that the combination of these parameters has big role in determining the stability of the system. In other words, these parameters have the most affect to the spread of COVID-19.

Geometrically, Fig. 3 shows the contour plot of basic reproduction number R_0 as a function of two parameters. The color bar placed in the right shows the value of R_0 , in other words it shows the height of the R_0 's surface. Since 1 is the critical point for R_0 that concludes the system's stability, then the interpretation of Fig. 3 can be done by observing the effect of changes in the parameters value on the R_0 value whether it makes R_0 approaching or leaving 1. Figs. 3a, 3b, and 3c, successively show that the combination of parameters Λ and β , p and β , d_1 and β have a dominant influence on increasing or decreasing the spread of COVID-19, whereas Figs. 3d, 3e, and 3f show that the combination of parameters p and Λ , d_1 and Λ , d_1 and p does not have a dominant effect on increasing or decreasing the spread of COVID-19.

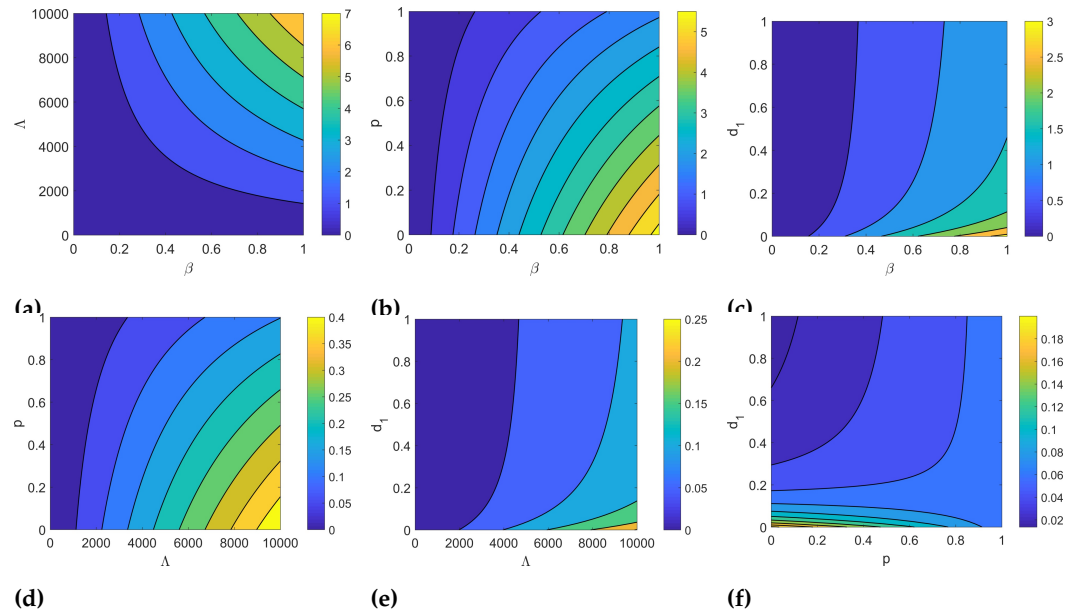


Figure 3. Contour plot of the basic reproduction number for the two combinations of parameters Λ , β , p , and d_1 .

4.3. Sensitivity Analysis of Parameters

Sensitivity analysis is performed to examine the effect of changes of the model's parameters to the dynamics of the model's compartments. Some papers have used this sensitivity technique in several research areas [36–38]. Suppose we have a vector of variables $\mathbf{X} = (S, I_h, I_c, Q_h, Q_H, R)^T$, a vector parameters $\mathbf{P} = (\Lambda, p, \beta, \nu, p_1, \mu, \alpha, d_1, \delta, \gamma, d_2, \eta)^T$, and a vector of the right-side of system (1) denoted by $\mathbf{F} = (\mathcal{F}, \mathcal{G}, \mathcal{H}, \mathcal{I}, \mathcal{J}, \mathcal{K})^T$, where $dS/dt = \mathcal{F}$, $dI_h/dt = \mathcal{G}$, $dI_c/dt = \mathcal{H}$, $dQ_h/dt = \mathcal{I}$, $dQ_H/dt = \mathcal{J}$, $dR/dt = \mathcal{K}$.

Define a sensitivity function $V = \frac{\partial \mathbf{X}}{\partial \mathbf{P}}$. Since \mathbf{X} contains \mathbf{P} and t , and \mathbf{F} contains \mathbf{X} and \mathbf{P} , then by doing total derivative for function V , we can derive a system of differential equations as follows

$$\frac{dV}{dt} = J(\mathbf{X})V + \frac{\partial \mathbf{F}}{\partial \mathbf{P}}, \quad (7)$$

where $J(\mathbf{X})$ is the Jacobian matrix 6×6 . There are six variables and twelve parameters. The size of matrix V is 6×12 and of matrix $\frac{\partial \mathbf{F}}{\partial \mathbf{P}}$ is 6×12 . Therefore, Equation (7) is a 6×12 matrix equation. If we pull out the elements of this matrix equation, we have a system with seventy-two (as many as the number of elements of V) plus six (number of elements of \mathbf{X}) differential equations.

For further writings, we denote $\frac{\partial S}{\partial \Lambda} = v_{\Lambda}^S$, $\frac{\partial S}{\partial p} = v_p^S$, $\frac{\partial S}{\partial \beta} = v_{\beta}^S$, \dots , $\frac{\partial S}{\partial \eta} = v_{\eta}^S$, and so on for the other variables. By solving the system (7) numerically, we can get solutions as the sensitivity of parameters over time. This time-dependent sensitivity is presented in Fig. 4. At any given time, we can observe the effect of each parameter changes to each variable. The positive value of the sensitivity means that if the parameter is raised then the variable goes higher, otherwise the negative value of the sensitivity means that if the parameter is raised then the variable goes lower, and the zero value of the sensitivity means that the changes of the parameter's value does not affect the variable at all.

Based on the sensitivity analysis in Fig. 4a, if the value of the parameter Λ increases, then the number of subpopulations R and S increases. In Figs. 4b, 4h, and 4k, the increase in values of the parameters p , d_1 , or d_2 results the increase in number of subpopulation Q_h and the decrease in number of subpopulations I_c or Q_H . In Fig. 4c, if the value of parameter β increases, then the number of subpopulations Q_h , Q_H , I_c , and I_h increases, but the number of subpopulations R and S decreases. In Figs. 4d and 4e, if the value of the parameters ν or p_1 increases, then the number of subpopulation R increases, but the number of subpopulation S decreases. In Fig. 4f, if the value of parameter μ increases,

then the number of subpopulations R and S decreases. In Fig. 4g, the increase in the value of parameter α results in the increase in the number of subpopulations R , I_c , and S , but the decrease in the number of subpopulation I_h . In Fig. 4i, if the value of parameter δ increases, then the number of subpopulations R , Q_H , and S increases, but the number of subpopulations I_c and Q_H decreases. In Figs. 4j and 4l, if the value of the parameters γ or η increases, then the number of subpopulation R increases, but the number of subpopulation Q_h decreases.

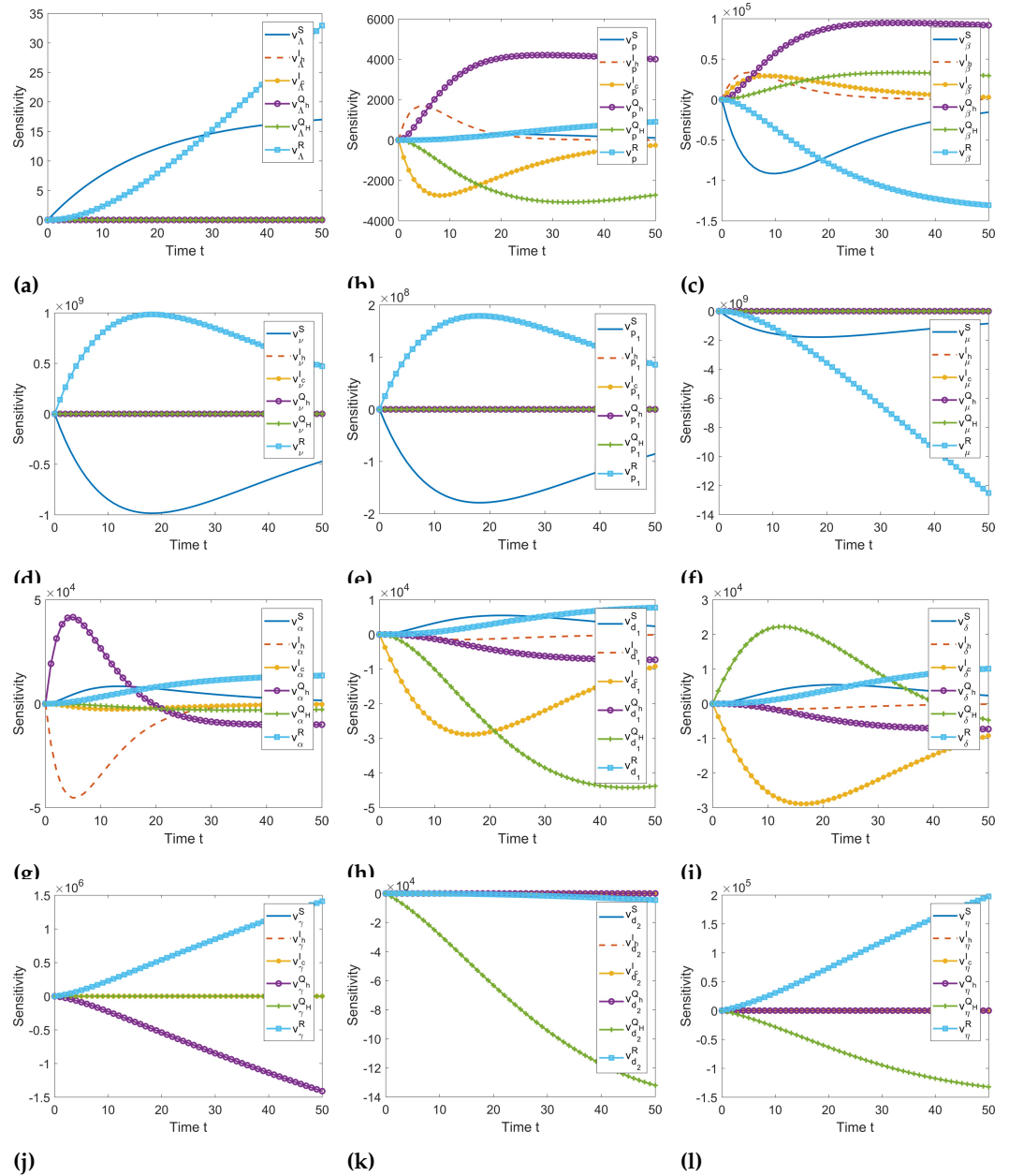


Figure 4. Time-dependent sensitivity of parameters to the variables. Panel (a) to (l) is the case of parameter Λ , p , β , v , p_1 , μ , α , d_1 , δ , γ , d_2 , η , respectively.

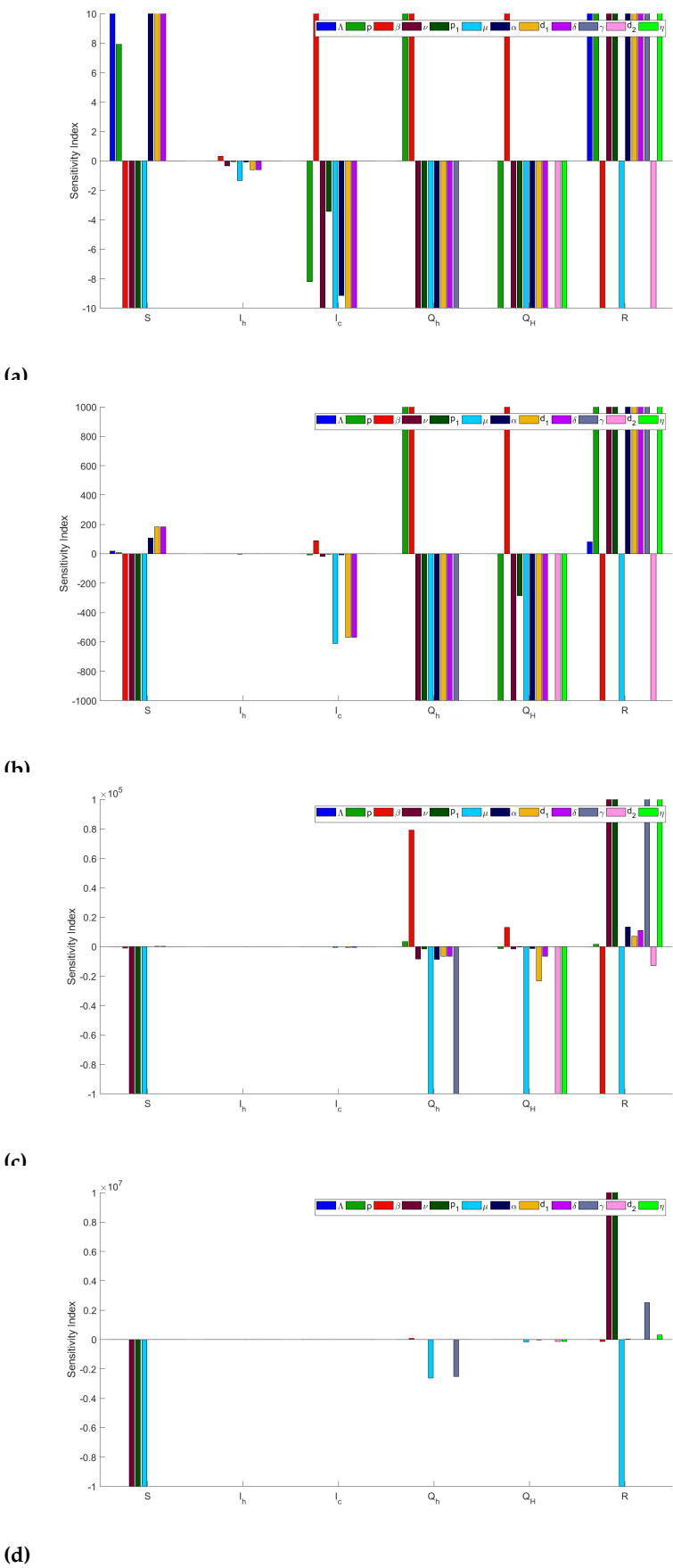


Figure 5. Sensitivity index after arriving at the equilibrium. Panel (a)-(d) is for the case of scale view $[-10, 10]$, $[-10^3, 10^3]$, $[-10^5, 10^5]$, $[-10^7, 10^7]$, respectively.

From Fig. 4, we can observe that some sensitivity has positive value at some first period, but at the next period the sensitivity value becomes negative or tends to zero. From these sensitivity graphs, especially at the peak point, we can observe the time when the parameter changes have the most effect to the variable. Therefore, another interesting result can be derived by observing the sensitivity index after arriving at the equilibrium. This can be done by taking the sensitivity values when the time is very long. By this method, we can determine which one of the parameters is the most sensitive to the model when converging to the equilibrium. In Fig. 5, we present the sensitivity index of all parameters for each variable. We give four different scales for depicting the sensitivity index, since some variables have values quite larger than other variables, thus it makes the sensitivity index has different level for each variable. From each panel of Fig. 5, we can observe that parameter μ , stands for natural death rate for each subpopulation, is the most sensitive parameter.

5. Discussion and Conclusion

This article explores the dynamic model of COVID-19 where infected individuals with comorbid disease are quarantined in hospitals provided by the local government and infected individuals without comorbid disease are self-isolated. Based on the results of the model analysis, the following are obtained: non-endemic and endemic equilibrium points; the basic reproduction number to determine whether the spread of COVID-19 is increasing or decreasing; the local asymptotic stability theorem of non-endemic equilibrium point; and the local and global asymptotic stability theorems of endemic equilibrium point.

According to the results of sensitivity analysis of the basic reproduction number using a contour plot, the parameters that their combination significantly impacts the system stability are recruitment rate of individuals entering the susceptible subpopulation, probability of infected individuals that have no comorbid disease, contact rate between the susceptible subpopulation with the infected subpopulation, and death rate of individuals infected with COVID-19. In addition, the combination of the contact rate with other three parameters produces wider range of COVID-19 spread. Therefore, minimizing contact rate is very good advise to be implemented in the government policy in order to reduce the disease contagion.

In addition, we provided sensitivity analysis to examine the effect of parameter changes on each subpopulation. From the visualization of the sensitivity function over time, we can observe the dynamical effect of each of parameter’s changes. We found, based on the sensitivity index after achieving equilibrium, that the natural death rate is the most sensitive parameter. The implication of this result is that the estimation of the natural death rate parameter must be done carefully in order to avoid transgression in depicting the true dynamics of the COVID-19 spread.

We also found that the symmetry aspects appear in the visualization of susceptible and recovered subpopulations over time, the image of some basic reproduction number sensitivity, and the depiction of some parameters sensitivity over time.

Author Contributions: Conceptualization, J.N. and M.F.A.; methodology, J.N. and M.F.A.; formal analysis, J.N.; investigation, J.N. and M.F.A.; resources, J.N.; writing—original draft preparation, J.N. and M.F.A.; writing—review and editing, J.N. and M.F.A.; visualization, M.F.A.; supervision, J.N. and M.F.A.; project administration, J.N.; funding acquisition, J.N. All authors have read and agreed to the published version of the manuscript.

Funding: The authors would like to thank Kemenristek Dikti providing Higher Education Grants of College Leading Basic Research for Fiscal Year 2022, contract no. 09/UN20.2.1/PG/DRPM/2022, through LPPM Universitas Cenderawasih who sponsored the research.

Institutional Review Board Statement: Not applicable.

Informed Consent Statement: Not applicable.

Data Availability Statement: Not applicable.

Conflicts of Interest: The authors declare no conflict of interest.

References

1. Ministry of Health Republic of Indonesia. Guidelines for Preparedness for Coronavirus Disease (COVID-19) (in Indonesian). *Ministry of Health RI Directorate General of Disease Prevention and Control (P2P)* **2020**, 11–12, 46–55.

2. Aguilar-Canto, F.J.; de León, U.A.P.; Avila-Vales, E. Sensitivity theorems of a model of multiple imperfect vaccines for COVID-19. *Chaos Solitons Fractals* **2022**, *156*, 111844.

3. Diagne, M.L.; Rwezaura, H.; Tchoumi, S.Y.; Tchuenche, J.M. A Mathematical Model of COVID-19 with Vaccination and Treatment. *Comput. Math. Methods Med.* **2021**.

4. Rana, P.S.; Sharma, N. The modeling and analysis of the COVID-19 pandemic with vaccination and treatment control: a case study of Maharashtra, Delhi, Uttarakhand, Sikkim, and Russia in the light of pharmaceutical and non-pharmaceutical approaches. *European Physical Journal: Special Topics* **2022**, 123.

5. Sasmita, N.R.; Ikhwan, M.; Suyanto, S.; Chongsuvivatwong, V. Optimal control on a mathematical model to pattern the progression of coronavirus disease 2019 (COVID-19) in Indonesia. *Global Health Research and Policy* **2020**, *5*(1).

6. Mandal, M.; Jana, S.; Nandi, S.K.; Khatua, A.; Adak, S.; Kar, T.K. A model based study on the dynamics of COVID-19: Prediction and control. *Chaos Solitons Fractals* **2020**, *136*, 109889.

7. Shen, Z.H.; Chu, Y.M.; Khan, M.A.; Muhammad, S.; Al-Hartomy, O.A.; Higazy, M. Mathematical modeling and optimal control of the COVID-19 dynamics. *Results Phys.* **2021**, *31*, 105028.

8. Nainggolan, J.; Fatmawati. Optimal prevention strategy of the type SIR covid-19 spread model in Indonesia. *Communications in Mathematical Biology and Neuroscience* **2021**, 1–13.

9. Nana-Kyere, S.; Boateng, F.A.; Jonathan, P.; Donkor, A.; Hoggar, G.K.; Titus, B.D.; Kwarteng, D.; Adu, I.K. Global Analysis and Optimal Control Model of COVID-19. *Comput. Math. Methods Med.* **2022** Jan 27, 9491847.

10. Ahmed, A.; Salam, B.; Mohammad, M.; Akgül, A.; Khoshnaw, S.H.A. Analysis coronavirus disease (COVID-19) model using numerical approaches and logistic model. *AIMS Bioengineering* **2020**, *7*, 130–146.

11. Arino, J.; Portet, S. A simple model for COVID-19. *Infectious Disease Modelling* **2020**, *5*, 309–315.

12. Arfan, M.; Lashin, M.M.A.; Sunthrayuth, P.; Shah, K.; Ullah, A.; Iskakova, K.; Gorji, M.R. On nonlinear dynamics of COVID-19 disease model corresponding to nonsingular fractional order derivative. *Medical & Biological Engineering & Computing* **2022**, *60*, 3169–3185.

13. Arfan, M.; Mahariq, I.; Shah, K.; Abdeljawad, T.; Laouini, G.; Mohammed, P.O. Numerical computations and theoretical investigations of a dynamical system with fractional order derivative. *Alexandria Engineering Journal* **2022**, *61*, 1982–1994.

14. Sugiyanto, S.; Abrori, M. A Mathematical Model of the Covid-19 Cases in Indonesia (Under and Without Lockdown Enforcement). *Biology, Medicine, & Natural Product Chemistry* **2020**, *9*, 15–19.

15. Khan, M.A.; Atangana, A.; Alzahrani, E.; Fatmawati. The dynamics of COVID-19 with quarantined and isolation. *Adv. Differ. Equations* **2020**, 2020.

16. Annas, S.; Pratama, M.I.; Rifandi, M.; Sanusi, W.; Side, S. Stability analysis and numerical simulation of SEIR model for pandemic COVID-19 spread in Indonesia. *Chaos Solitons Fractals* **2020**, 139.

17. Fitriani, U.A.; Widowati; Sutimin; Sasongko, P.S. Mathematical modeling and analysis of COVID-19 transmission dynamics in Central Java Province, Indonesia. *Journal of Physics: Conference Series* **2021**, 1943.

18. Anggriani, N.; Ndi, M.Z.; Amelia, R.; Suryaningrat, W.; Pratama, M.A.A. A mathematical COVID-19 model considering asymptomatic and symptomatic classes with waning immunity. *Alexandria Eng. J.* **2022**, *61*, 113–124.

19. Okuonghae, D.; Oname, A. Analysis of a mathematical model for COVID-19 population dynamics in Lagos, Nigeria. *Chaos Solitons Fractals* **2020**, *139*, 110032.

20. Kifle, Z.S.; Obsu, L.L. Mathematical modeling for COVID-19 transmission dynamics: A case study in Ethiopia. *Results Phys.* **2022**, *34*, 105191.

21. Asempapa, R.; Oduro, B.; Apenteng, O.O.; Magagula, V.M. A COVID-19 mathematical model of at-risk populations with non-pharmaceutical preventive measures: The case of Brazil and South Africa. *Infectious Disease Modelling* **2022**, 7.

22. Postnikov, E.B. Estimation of COVID-19 dynamics “on a back-of-envelope”: Does the simplest SIR model provide quantitative parameters and predictions? *Chaos Solitons Fractals* **2020**, *135*, 109841.

23. Ivorra, B.; Ferrández, M.R.; Vela-pérez, M.; Ramos, A.M. Mathematical modeling of the spread of the coronavirus disease 2019 (COVID-19) taking into account the undetected infections. The case of China. *Commun Nonlinear Sci Numer Simul* **2020**, *88*, 105303.

24. Yang, C.; Wang, J. A mathematical model for the novel coronavirus epidemic in Wuhan, China. *Math. Biosci. Eng.* **2020**, *17*, 2708–2724.

25. Barmparis, G.D.; Tsironis, G.P. Estimating the infection horizon of COVID-19 in eight countries with a data-driven approach. *Chaos Solitons Fractals* **2020**, 135.

26. Sreeramula, S.; Rahardjo, D. Estimating COVID-19 R t in Real-time: An Indonesia health policy perspective. *Mach. Learn. Appl.* **2021**, *6*, 10036.

27. Mekonen, K.G.; Balcha, S.F.; Obsu, L.L.; Hassen, A. Mathematical Modeling and Analysis of TB and COVID-19 Coinfection. *J. Appl. Math.* **2022**.

28.

Ssebuliba, J.; Nakakawa, J.N.; Ssematimba, A.; Mugisha, J.Y.T. Mathematical modelling of COVID-19 transmission dynamics in a partially comorbid community. *Partial Differ. Equations Appl. Math.* **2022**, *5*, 100212.

318

29.

Das, P.; Upadhyay, R.K.; Misra, A.K.; Rihan, F.A.; Das, P.; Ghosh, D. Mathematical model of COVID-19 with comorbidity and controlling using non-pharmaceutical interventions and vaccination. *Nonlinear Dyn.* **2021**, *106*, 1213–1227.

319

30.

Sanyaolu, A.; Okorie, C.; Marinkovic, A.; Patidar, R.; Younis, K.; Desai, P.; Hosein, Z.; Padda, I.; Mangat, J.; Altaf, M. Comorbidity and its Impact on Patients with COVID-19. *SN Compr. Clin. Med.* **2020**, *2*, 1069–1076.

320

31.

Okyere, S.; Ackora-Prah, J. A Mathematical Model of Transmission Dynamics of SARS-CoV-2 (COVID-19) with an Underlying Condition of Diabetes. *Int. J. Math. Math. Sci.* **2022**, 1–15.

321

32.

Diekmann, O.; Heesterbeek, J. Mathematical Epidemiology of Infectious Diseases. *Wiley Series in Mathematical and Computational Biology* **2000**.

322

33.

Van Den Driessche, P.; Watmough, J. Reproduction numbers and sub-threshold endemic equilibria for compartmental models of disease transmission. *Math. Biosci.* **2002**, *180*, 29–48.

323

34.

Li, M.T.; Jin Z.; Sun, G.Q.; Zhang, J. Modeling direct and indirect disease transmission using multi-group model. *J. Math. Anal. Appl.* **2017**, *446*, 1292–1309.

324

35.

La Salle, J.P. Stability theory for ordinary differential equations. *J. Differ. Equations* **1968**, *4*, 57–65.

325

36.

Suandi, D.; Ningrum, I.P.; Alifah, A.N.; Izzah, N.; Reza, M.P.; Muwahidah, I.K. Mathematical Modeling and Sensitivity Analysis of the Existence of Male Calico Cats Population Based on Cross Breeding of All Coat Colour Types. *Commun. Biomath. Sci.* **2019**, *2*, 96–104.

326

37.

Ansori, M.F. Mathematical model and its application for analyzing macroprudential instrument in the banking industry (in Indonesian). Doctoral Dissertation, Institut Teknologi Bandung, Bandung, Indonesia, 26 November 2021.

327

38.

Sunarsih; Ansori, M.F.; Khabibah, S.; Sasongko, D.P. Continuous and Discrete Dynamical Models of Total Nitrogen Transformation in A Constructed Wetland: Sensitivity and Bifurcation Analysis. *Symmetry* **2022**, *14*, 1924.

328

329

330

331

332

333

334

335

336

337

338

339